Article

Journal of the Brazilian Chemical Society

https://dx.doi.org/10.21577/0103-5053.20230108

J. Braz. Chem. Soc. **2024**, *35*, 2, e-20230108, 1-10

Use of High-Efficiency Lignocellulose-Based Materials for Toxic Ions Removal: Impact of Surface Chemistry and Mathematical Modeling

Diego Q. Melo,[a] Lucas F. Amorim,[b] Juliene T. Oliveira,[b] João A. N. da Cunha Junior,[a] André H. B. de Oliveira,[b] André G. de Oliveira,[b,c] Carla B. Vidal*,[d] and Ronaldo F. do Nascimento[b]

[a]*Instituto Federal de Educação, Ciência e Tecnologia do Sertão Pernambucano (IFSertão), PE 647, km 22, PISNC N-4, Campus Petrolina Zona Rural, 56302-970 Petrolina-PE, Brazil*

[b]*Departamento de Química Analítica e Físico-Química, Universidade Federal do Ceará (UFC), Campus do Pici, Bl. 940, 60451-970 Fortaleza-CE, Brazil*

[c]*Centro de Ciências Tecnológicas, Universidade de Fortaleza (UNIFOR), Av. Washington Soares, 1321, Edson Queiroz, 60881-905 Fortaleza-CE, Brazil*

[d]*Departamento de Química e Biologia, Universidade Tecnológica Federal do Paraná (UTFPR), Rua Deputado Heitor Alencar Furtado, 5000, Cidade Industrial, 81280-340 Curitiba-PR, Brazil*

Low-cost adsorbents promote the valorization of locally sourced waste materials and are still a significant challenge for removing toxic metal ions from industrial effluents. In this sense, Castor (*Ricinus communis* L.) stalks (CS) were activated with an alkaline solution and tested as an adsorbent to remove nickel, copper, cadmium, and lead ions. A 2^{4-1} factorial design was carried out and showed a correlation and influence of the variables, such as pH, adsorbent mass, agitation rate, and initial concentration in the adsorption process. The adsorbents in their natural, activated, and saturated states were characterized. After activation, X-ray diffraction results revealed a change from cellulose I to cellulose II. The X-ray fluorescence showed that the ion exchange adsorption mechanism occurred. For the kinetic adsorption studies, the equilibrium time was reached up to 15 min. Different isotherm models described the adsorption process, with the Sips model providing the best fit to the experimental data. Five cycles of sorption/desorption using 0.1 mol L^{-1} HCl elution were carried out with a minimal loss in sorption capacity and physical degradation. Nickel and copper ions exhibited the lowest desorption rates. Due to their efficiency, CS can be a promising and low-cost alternative for removing metal ions.

Keywords: adsorption, metals, biomass, pollutants, environmental, factorial design

Introduction

The rapid population growth added to intensive industrial development has led to an increase in environmental pollution levels. Inadequate industrial waste disposal generates large amounts of toxic pollutants, such as toxic metals, nonmetals, radionuclides, and various organic contaminants in the air, soil, and water matrices. Their presence has multiple impacts on the environment and health of living things, mainly due to their stability, high solubility, and extensive migration activity. Thus, it is necessary to remove them from wastewater.[1,2]

Among the listed pollutants, toxic metals are noteworthy for being primarily used in many industries, such as batteries, leather, electrical, electroplating, fertilizers, pesticides, mining, ore refining, etc.[3] Given the dangerous effects, persistence, and accumulation, they represent a class of pollutants with a high risk to human and environmental health.[4,5]

Human exposure to these pollutants can cause damage even at low concentrations. Therefore, removing toxic metal ions from aqueous solutions is extremely important. Several technologies have been developed for the decontamination of wastewater, such as chemical precipitation, ion exchange, electrochemical methods, filtration, and adsorption using activated carbon.[6,7]

However, most existing technologies are often expensive or ineffective for removing pollutants at low levels (electrochemical methods, filtration). Moreover,

*e-mail: cvidal@utfpr.edu.br
Editor handled this article: Fernando C. Giacomelli (Associate)

some methods have disadvantages, such as producing highly toxic sludge (ex., chemical precipitation). The adsorption process is a technique that is gaining prominence in the current research, mainly for simplicity, especially when agro-industrial byproducts and waste are used as adsorbents, increasing the life cycle of these materials.[8]

Recent studies[9-12] show that lignocellulosic adsorbents have great potential to remove heavy metals from aqueous solutions. Several factors influence the adsorption processes, such as the type and concentration of metal ions, the pH, the contact time, and the initial concentration of adsorbent.[13] Different isotherms and chemical modifications of the adsorbents have been explored to improve their adsorption capacity and selectivity.[14-17] Moreover, the chemical characterization of solid agroforestry residues, aiming at their utilization as adsorbents for metals in water, has been a subject of interest in recent years.[18] These studies highlight the potential of lignocellulosic adsorbents as a low-cost and sustainable solution for removing heavy metals from aqueous solutions.[1,3,9-12,19,20]

In general, the adsorption process using biomass-derived materials as adsorbents can significantly reduce capital and operating costs and, thus, the total wastewater treatment costs, in addition to promoting a positive impact on the environment since the destination of these materials is highly dangerous to the environment.[21,22] *Ricinus communis* L. cultivation waste is hugely abundant and inexpensive, which led the team to conduct in-depth studies to ascertain its potential.

In this context, the present study aimed to evaluate the conversion of agricultural waste from the cultivation of *Ricinus communis* L. into a low-cost and efficient adsorbent for removing toxic heavy metals from contaminated water sources.

The novelty of this study lies in the valorization of waste and its potential as adsorbent for wastewater treatment. The study investigated the effect of various parameters, including initial metal concentration, adsorbent dosage, contact time, and pH, on the efficiency of the adsorption process. The results demonstrated the agricultural waste's high potential as an adsorbent, with a higher adsorption capacity than many other reported adsorbents. The findings of this study provide an alternative solution for the disposal of agricultural waste, promoting sustainability and circular economy principles.

Experimental

Adsorbent and chemicals

Castor (*Ricinus communis* L.) stalk (CS) residues were provided from Embrapa, located in Ceará, Brazil. Mono and multielement stock solutions of Ni^{II}, Cu^{II}, Cd^{II}, and Pb^{II} (1000 mg L^{-1}) were prepared with $Ni(NO_3)_2.6H_2O$, $Cu(NO_3)_2.3H_2O$, $Cd(NO_3)_2.4H_2O$ and $Pb(NO_3)_2$ (Merck, São Paulo, Brazil), respectively. Standard solutions were prepared in acetate buffer solution at adequate pH.

Activation and characterization of the adsorbent

0.5 kg of CS was added to suitable flasks containing different alkaline solution concentrations (5, 7, 10, and 15% m/v) prepared by mixing 1 liter of ultra-pure water and the respective amounts of alkaline solution. The flasks were agitated for 4 h at 150 rpm and 60 °C while the ambient temperature was maintained at 28 ± 2 °C. The characterization of the adsorbents before and after activation were performed using the Fourier transform infrared spectroscopy (FTIR) technique with a Brucker spectrometer (Vetex ALPHA II model) and ATR Miracle accessory, diamond crystal covered with zinc selenide, in the range 4000-400 cm^{-1}, X-ray diffraction, and X-ray fluorescence (model ZMS MiniII, Rigaku, Tokyo, Japan) techniques. Diffractograms were obtained using a Rigaku diffractometer (model DMAXB, Tokyo, Japan) with angular variation (2θ) from 5 to 30° and Cu Kα radiation.

Adsorption and experimental design

To study the effect of pH, metal ion concentration, agitation (rpm), and adsorbent mass on the adsorption batch system, a 2^{4-1} fractional factorial design[23] of metal ions was carried out according to Melo *et al.*[24] methodology (Table 1).

Table 1. Coded factors used in the 2^{4-1} fractional factorial design for studying the adsorption of Cu^{II}, Pb^{II}, Ni^{II}, and Cd^{II} on alkaline CS

Code	Factor	(–)	0	(+)
A	pH	4.5	5.0	5.5
B	adsorbent mass / mg	50	100	150
C	agitation rate / rpm	100	150	200
D	initial metal concentration / (mg L^{-1})	100	300	500

CS: Castor (*Ricinus communis* L.) stalks.

The adsorption tests were carried out by adding 25 mL of multielementary solutions of Ni^{II}, Cu^{II}, Cd^{II}, and Pb^{II} ions in 50 mL flasks with the alkaline CS adsorbents for 2 h at 28 ± 2 °C. The responses q (adsorption capacity) and q_{tot} (total adsorption capacity) were obtained for each experiment of planning 2^{4-1}, equations 1 and 2.[24,25]

$$q = \frac{(C_0 - C_e)V}{W} \quad (1)$$

$$q_{tot} = \sum_{j=1}^{4} \frac{\left(C_{0,j} - C_{e,j}\right)}{W} V \quad (2)$$

where $C_{e,j}$ is the equilibrium metal ion concentration (mg L^{-1}), W is the mass of the adsorbent (g), $C_{0,j}$ is the initial concentration of the metal ion (mg L^{-1}), and V is the volume of the solution (L). The 2^{4-1} fractional experiment results were analyzed using Minitab Statistical Software (version 17).[26] Adsorption tests (kinetics and isotherms) were performed after determining the condition of the fractional design.

Adsorption studies

Kinetic studies were performed in duplicate from 0 to 60 min to determine the adsorption equilibrium time in multielement systems with the following conditions CS 15%; W = 0.05 g; T = 28 ± 2 ºC, pH = 5.5.

To study the contribution of the mass transfer parameter to the adsorption kinetics, the homogeneous solid diffusion model (HSDM), which models mass transfer in the solid as diffusion in an amorphous and homogeneous sphere, was used. HSDM equation describing homogeneous diffusion in a sphere, assuming constant diffusivity, D_s, at all points in the particle is shown at equation 3, where r is the radial position (cm), and q the adsorption quantity of solute in the solid (mg g^{-1}) varying with radial position at time t.[27]

$$\frac{\partial q}{\partial t} = \frac{D_s}{r^2} \frac{\partial}{\partial r}\left(r^2 \frac{\partial q}{\partial r}\right) \quad (3)$$

Considering an infinite bath process in which the adsorbent sphere is free of the solution, the concentration of solute at the surface remains constant, and external film resistance is negligible, equation 3 can be solved into equation 4 by the separation-of-variables technique.[28]

$$\frac{q}{q_s} = 1 + \frac{2R}{\pi r} \sum_{n=1}^{\infty} \frac{(-1)^n}{n} \sin\frac{n\pi r}{R} \exp\left(\frac{-D_s n^2 \pi^2 t}{R^2}\right) \quad (4)$$

where R is the total particle radius and n is number of measurements. To obtain the average value of q in a spherical particle, denoted by $\bar{q}$, equation 5, where q(r) represents the local value of the solid-phase concentration. Inserting the solution for q(r) into equation 4,[28] developed equation 6 for the average concentration in the solid at infinite time, q_∞.

$$\bar{q} = \frac{3}{R^3} \int_0^R q(r) r^2 dr \quad (5)$$

$$\frac{\bar{q}}{q_\infty} = 1 - \frac{6}{\pi^2} \sum_{n=1}^{\infty} \frac{1}{n^2} \exp\left(\frac{-D_s n^2 \pi^2 t}{R^2}\right) \quad (6)$$

For small times, or, more precisely, $q/q_\infty < 0.3$, this last equation may be written as:

$$\frac{\bar{q}}{q_\infty} = 6\left(\frac{D_s t}{R^2}\right)^{1/2} \left[\pi^{-1/2} + L\right] \quad (7)$$

Thus, a plot of $\frac{\bar{q}}{q_\infty}$ *vs*. the square root of time should give a straight line of slope $6\left(\frac{D_s}{\pi R^2}\right)^{1/2}$, from which D_s can be determined. The concentration profiles obtained in the kinetic assays (metal ion concentration in the liquid *vs*. time) were employed, and the q_∞ (equilibrium adsorption capacity) values were determined from equation 1.

To carry out the adsorption isotherm experiments in mono- and multielement systems, 25 mL of these solutions were used with concentrations ranging from 20 to 500 mg L^{-1} in 50 mL conical flasks. The studies were performed in triplicate. The experimental data obtained were subjected to Langmuir, Freundlich, and Sips adsorption isotherms (Table 2).

Table 2. Isotherm models

Isotherm model	Equation	Parameter
Langmuir isotherm[29]	$q = \frac{q_{max} K_L C_e}{1 + K_L C_e}$	q: amount of metal adsorbed *per* unit mass of adsorbent (mg g^{-1}); q_{max}: adsorbent's maximum adsorption capacity (mg g^{-1}); K_L: equilibrium constant Langmuir (L mg^{-1}); C_e: ion concentration in equilibrium solution (mg L^{-1})
Freundlich isotherm[30]	$q = K_F C_e^{1/n}$	K_F: Freundlich adsorption isotherm constant; n: adsorption intensity constant
Sips isotherm[31]	$q = \frac{q_{max}(K_S C_e)^{1/n_S}}{1 + (K_S C_e)^{1/n_S}}$	K_s: Sips adsorption isotherm constant

Desorption study

The desorption characteristics of previously adsorbed metal ions on CS (monoelement system) were tested by various desorption eluents (10 mL), such as 0.1 M HCl solution, ultrapure water, and acetate buffer solution pH 5.5. Five cycles of batch adsorption-desorption were carried out on the same adsorbent. Quantifying the concentration of metal ions before and after elution made it possible to determine the removal percentage in each cycle.

Results and Discussion

Influence of alkaline treatments

Figure 1 shows the adsorption capacity results after the activation of CS under different NaOH concentrations.

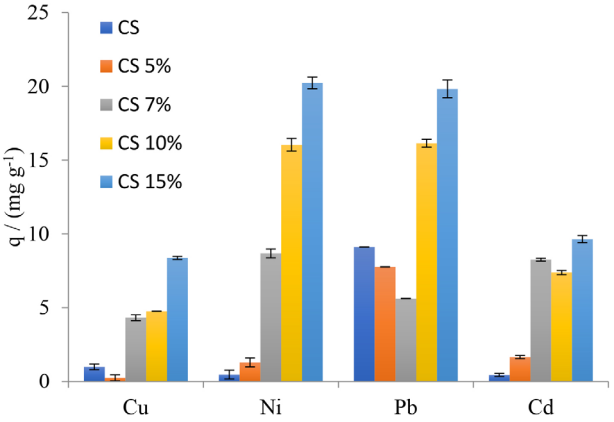

Figure 1. Adsorption capacities (mg g^{-1}) of metal ions *versus* concentration levels. Initial conditions: dose adsorbent (2.0 g L^{-1}), concentration (100 mg L^{-1}), contact time (4 h), pH (5.5), and temperature (28 ± 2 °C).

The results show that the activation of CS with 15% NaOH solution presented better adsorption capacities (mg g^{-1}) for all studied ions (9.65, 8.37, 20.4, and 19.83 for Cd^{II}, Cu^{II}, Ni^{II} and Pb^{II}, respectively). Thus, CS 15% was chosen in the following experiments.

Alkaline solutions promote changes in the structure and morphology of lignocellulosic adsorbents. The abundant hydroxyl sites in cellulose are often unavailable for adsorption due to binding with the lignin and hemicellulose components. The dissolution and removal of these components increase the availability and access to hydroxyl sites, increasing the efficiency of the adsorbent. In addition, the activation caused the conversion of type I into type II cellulose due to the breaking of intra- and intermolecular bonds present in the cellulose (Figure 2). This irreversible conversion makes the material more thermodynamically stable.[32]

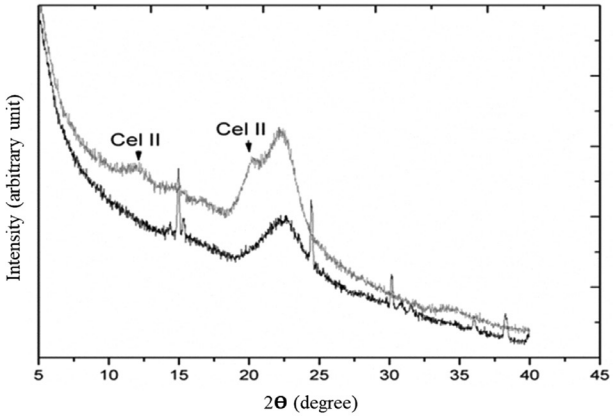

Figure 2. X-ray diffraction of adsorbents. Black (CS), gray (CS 15%).

Experimental design and statistical analysis

The results of each test for multielement metal ion adsorption provide different adsorption using CS 15% capacity values for each metal, which makes it possible to choose an experimental condition to favor a particular metal ion adsorption, as shown in Table 3.

Pareto charts are necessary to verify whether the results of the interaction effects present significance at the levels studied (Figure 3).

The A (pH) effect is not significant for q_{NiII} and q_{PbII}. The D (initial concentration) effect is not significant for q_{NiII}; the values of the studied range do not influence the response. On the other hand, all effects were significant for q_{CuII} and q_{CdII}. These data provide results for choosing the best experimental conditions for a given pollutant ion in multi-elementary systems. On the other hand, it also makes it possible to evaluate the best experimental condition (q_{tot}) for removing all metal ions (Figure 4).

Only the main B (adsorbent mass) effect affects the

Table 3. Fractional factorial design (2^{4-1}) and experimental values for multielement metal ions adsorption

Run	Coded factors								
	A	B	C	D[a]	q_{CuII} / (mg g^{-1})	q_{PbII} / (mg g^{-1})	q_{NiII} / (mg g^{-1})	q_{CdII} / (mg g^{-1})	q_{tot} / (mg g^{-1})
1	–	–	–	–	16.82 ± 0.20	30.40 ± 0.62	3.78 ± 0.31	1.66 ± 0.26	52.66 ± 2.72
2	+	–	–	+	27.40 ± 0.39	70.16 ± 0.82	2.86 ± 0.51	9.66 ± 0.20	110.1 ± 1.26
3	–	+	–	+	5.57 ± 0.94	46.40 ± 0.20	3.86 ± 0.51	0.45 ± 0.14	56.28 ± 5.69
4	+	+	–	–	12.17 ± 0.21	17.17 ± 0.05	3.41 ± 0.49	2.34 ± 0.45	35.10 ± 1.92
5	–	–	+	+	30.63 ± 0.98	78.83 ± 0.61	6.84 ± 0.52	1.22 ± 0.00	117.5 ± 1.83
6	+	–	+	–	16.79 ± 0.69	30.35 ± 0.65	7.890 ± 0.42	3.63 ± 0.52	96.21 ± 1.97
7	–	+	+	–	12.42 ± 0.53	16.60 ± 0.06	0.850 ± 0.10	0.81 ± 0.00	30.68 ± 1.17
8	+	+	+	+	15.65 ± 0.43	52.76 ± 0.85	2.10 ± 0.00	1.82 ± 0.00	72.27 ± 0.69
9	0	0	0	0	23.25 ± 0.82	20.72 ± 0.97	4.10 ± 0.92	0.54 ± 0.07	48.61 ± 1.86

[a]Generator: I: ABCD; A: pH effect; B: adsorbent mass effect; C: agitation rate effect; D: initial metal concentration. q: amount of metal adsorbed *per* unit mass of adsorbent.

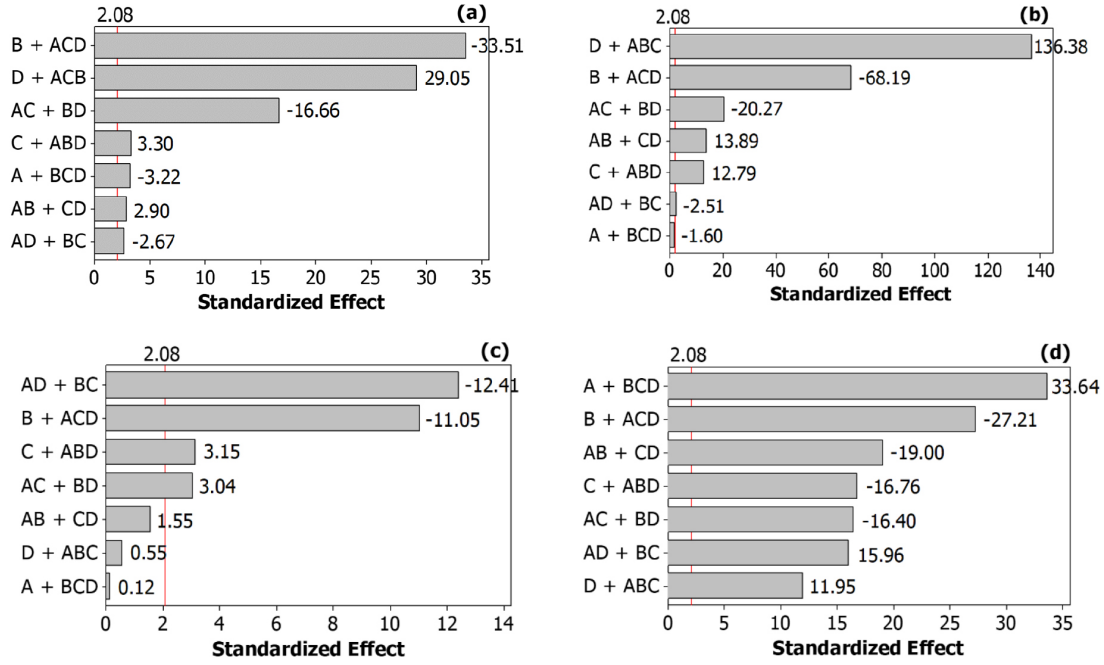

Figure 3. Standardized Pareto charts showing the main effects of experimental parameters on responses at the confidence limit of 95% for (a) q_{CuII}, (b) q_{PbII}, (c) q_{NiII}, and (d) q_{CdII}. A: pH effect; B: adsorbent mass effect; C: agitation rate effect and D: initial metal concentration.

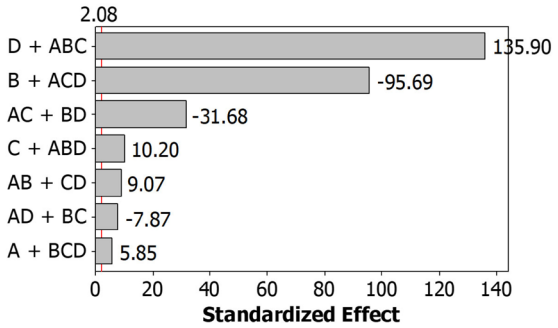

Figure 4. Standardized Pareto charts show experimental parameters' main effects on responses at the confidence limit of 95% for q_{tot}. A: pH effect; B: adsorbent mass effect; C: agitation rate effect and D: initial metal concentration.

response negatively. That is, the higher the value is, the lower the response (q_{tot}). This result shows that alkaline CS has a large number of active sites for adsorption. The main effects A (pH), C (adsorption rate), and D (initial concentration) positively affect the response; that is, the higher the pH is, the better the adsorption capacities obtained. The attraction of metal ions to the adsorbent increases as the surface charge of the adsorbent becomes increasingly negative.

Higher initial metal ions concentrations and higher agitation rates favor the metal ions migration from the solution to the CS 15% surface. Higher agitation rates tend to reduce the film around the adsorbent, and higher concentrations of pollutant ions increase the concentration gradient, favoring adsorption.[33] Similar results were found by Nouacer *et al.*[34]

Tables 4 and 5 present the significance tests performed to evaluate the results of the models obtained. They show

Table 4. Analysis of variance (ANOVA) for each metal capacity adsorption

Source	DF	q_{CuII}				q_{PbII}				q_{NiII}				q_{CdII}			
		SS	MS	*F*	*P*	SS	MS	*F*	*P*	SS	MS	*F*	*P*	SS	MS	*F*	*P*
Model	8	1088.43	136.05	317.67	0.000	13777.30	1722.16	3619.97	0.000	982.582	122.823	37.32	0.000	208.78	26.10	444.98	0.000
A	1	4.44	4.44	10.36	0.004	1.22	1.22	2.55	0.125	0.0048	0.0048	0.01	0.905	66.36	66.36	1131.43	0.000
B	1	480.80	480.80	1122.61	0.000	2212.26	2212.26	4650.15	0.000	401.442	401.442	121.99	0.000	43.41	43.41	740.18	0.000
C	1	4.68	4.68	10.92	0.003	77.78	77.78	163.50	0.000	32.625	32.625	9.91	0.005	16.47	16.47	280.89	0.000
D	1	361.46	361.46	843.96	0.000	8849.04	8849.04	18600.59	0.000	0.0990	0.0990	0.30	0.589	8.38	8.38	142.82	0.000
AB	1	3.60	3.60	8.40	0.009	91.75	91.75	192.86	0.000	0.7865	0.7865	2.39	0.137	21.17	21.17	360.87	0.000
AC	1	118.80	118.80	277.39	0.000	195.48	195.48	410.89	0.000	30.373	30.373	9.23	0.006	15.77	15.77	268.84	0.000
AD	1	3.06	3.06	7.15	0.014	2.99	2.99	6.28	0.021	507.009	507.009	154.08	0.000	14.93	14.93	254.64	0.000
Curvature	1	111.59	111.59	260.56	0.000	2346.78	2346.78	4932.91	0.000	0.2230	0.2230	0.68	0.420	22.30	22.30	380.16	0.000
Pure error	21	8.99	0.43			10.00	0.48			69.104	0.3291			1.23	0.06		

q_{CuII}: $R^2 = 0.9918$, $R^2_{adj} = 0.9887$; q_{PbII}: $R^2 = 0.9993$, $R^2_{adj} = 0.9990$; q_{PNiII}: $R^2 = 0.9343$, $R^2_{adj} = 0.9093$; q_{CdII}: $R^2 = 0.9941$, $R^2_{adj} = 0.9919$. q: amount of metal adsorbed *per* unit mass of adsorbent; DF: degrees of freedom; SS; sum of square; MS: mean square; R^2_{adj}: adjusted coefficient of determination; R^2: coefficient of determination.

Table 5. Analysis of variance (ANOVA) for q_{tot}

Source	Sum of squares	DF	Mean square	*F*	*P*
Model	22945.4	8	2868.2	3916.74	0.000
A	25.1	1	25.1	34.23	0.000
B	6705.4	1	6705.4	9156.75	0.000
C	76.2	1	76.2	104.07	0.000
D	13523.4	1	13523.4	18467.34	0.000
AB	60.2	1	60.2	82.27	0.000
AC	734.9	1	734.9	1003.57	0.000
AD	45.4	1	45.4	61.94	0.000
Curvature	1774.9	1	1774.9	2423.75	0.000
Pure error	15.4	21	0.7		

R^2 = 0.9993, R^2_{adj} = 0.9991. q: amount of metal adsorbed *per* unit mass of adsorbent. DF: degrees of freedom; R^2_{adj}: adjusted coefficient of determination; R^2: coefficient of determination.

correlations between factors and responses, corroborated by the significance of the models (p = 0.05) presented in analysis of variance (ANOVA). The R^2 values at a 95% confidence level were 0.9990 for q_{PbII}, 0.9887 for q_{CuII}, 0.9083 for q_{NiII}, 0.9919 for q_{CdII} and 0.991 for q_{tot}, confirming the high correlation between the observed and predicted values.[34]

Table 6 presents the regression equations of the fitted models in terms of coded values. These equations are essential due to the possibility of estimating adsorption capacity results within the studied range. For example, q_{CuII} in a multielement system can be obtained by keeping the adsorbent mass and pH values at the lowest level (–1) and the adsorption rate and initial concentration values at the highest level (+1) (Figure 3a).

Table 6. Regression equations of the fitted models in terms of coded values

q_{CuII} = 18.43 – 0.43*A – 4.48*B + 0.44*C + 3.88*D + 0.39*A*B – 2.23*A*C – 0.36*A*D + 4.82*CtPt
$q_{Pb(II}$ = 42.84 – 9.60*B + 1.80*C + 19.20*D + 1.96*A*B – 2.85*A*C – 0.35*A*D – 22.11*CtPt
q_{NiII} = 3.85 – 1.29*B + 0.37*C + 0.36*A*C – 1.45*A*D
q_{CdII} = 2.70 + 1.66*A – 1.35*B – 0.83*C + 0.59*D – 0.94*A*B – 0.81*A*C + 0.79*A*D – 2.16*CtPt
q_{tot} = 67.81 + 1.02*A – 16.71*B + 1.78*C + 23.74*D + 1.58*A*B – 5.53*A*C – 1.37*A*D – 19.23*CtPt

A: pH; B: adsorbent mass; C: agitation rate; D: initial metal concentration; CtPt: central point.

As a result, we obtained a value of 30.64 mg g^{-1}, similar to experiment 5 (Table 3), confirming the model's accuracy. Furthermore, including the central point in the experimental design created the term CtPt, which indicates curvature in the model, exhibiting nonlinearity between the correlated variables.

Adsorption kinetics

The equilibrium times for the adsorption of metal ions onto CS 15% were 8 min for Cu^{II} and 15 min for Ni^{II}, Cd^{II}, and Pb^{II} (Figure 5).

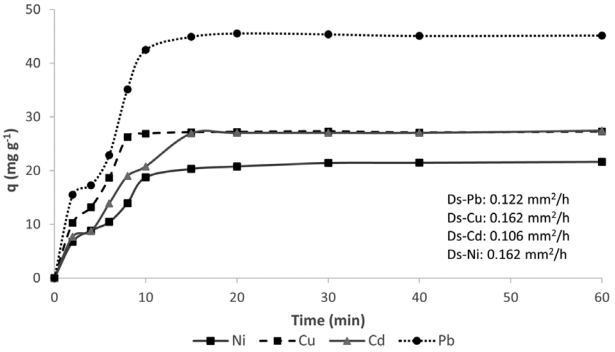

Figure 5. Multielement adsorption kinetics for CS 15%. W = 0.05 g; C_o = 100 mg L^{-1}; T = 28 ± 2 ºC; pH = 5.5.

The adsorption kinetics studies revealed rapid adsorption of metal ions, 8 min for Cu^{II} and 15 min for the other ions. Many active sites in the adsorbent and the high concentration of metal ions in the medium can explain the fast initial adsorption. These favorable conditions increase the probability of contact and interaction between the metal ions and the functional groups of the adsorbent, allowing for more efficient and rapid adsorption.[34,35]

From the equilibrium time obtained in the adsorption kinetics, it was possible to evaluate the removal of Ni^{II}, Cu^{II}, Cd^{II}, and Pb^{II} under the influence of their respective concentrations in mono-elementary solution and observe the efficiency of the adsorbent. The results demonstrate excellent adsorption potential for CS 15%, removing 100% for Pb^{II}, 73.15% for Cu^{II}, 55.14% Cd^{II}, and 51.0% Ni^{II} from an initial concentration of 20 mg L^{-1}, Figure 6.

Adsorption isotherms

In this study, tests were carried out in both mono and multielement system (Figure 7).

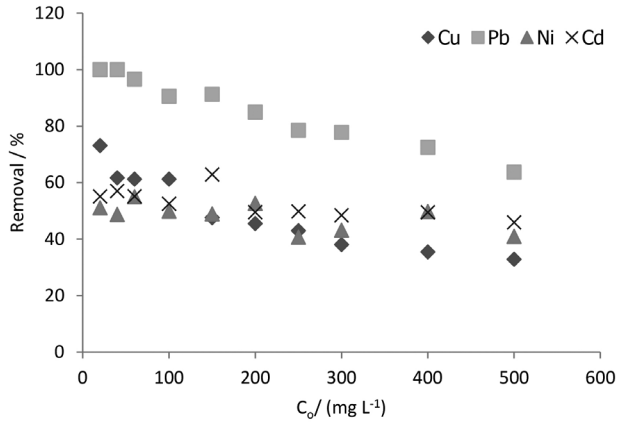

Figure 6. Effect of the initial concentration of Ni^{II}, Cu^{II}, Cd^{II}, and Pb^{II} on CS 15%. W = 0.05 g; C_o = 20 mg L^{-1}; T = 28 ± 2 ºC; pH = 5.5.

In a multielement system, metal ion adsorption capacities were suppressed; adsorption capacities were lower than in the monoelement system, suggesting a competition effect for the adsorption sites. However, the total adsorption capacity of metal ions (Ni, Cu, Cd, and Pb) in a multielement system is 200.89 mg g^{-1}. On the other hand, Pb^{II} in a mono-element system was 175 mg g^{-1}, very close to q_{tot} in a multielement system. The highest value in this system is due to the high concentration gradient, which is approximately four times greater.[34,35]

Figure 7 shows that the adsorption capacities of Ni, Cu, Cd, and Pb ions in the two types of systems (mono and multielement) are similar at low concentrations, suggesting specific sites and no adsorption competition since there is excellent availability of binding sites in the early times of the process. However, Pb^{II} adsorption was observed to be an intense competition, significantly reducing its adsorption capacity in a multielement system.[36]

The experimental adsorption capacities (mg g^{-1}) in the CS 15% in mono-elementary and multi-elementary systems follow the order Pb (175.1) > Cd (124.8) > Ni (111.1) > Cu (89.23) and Cu (56.78) > Pb (55.82) > Cd (44.72) > Ni (43.48), respectively. Similar results were found by Neris *et al.*[9]

Langmuir, Freundlich, and Sips adsorption isotherms were used to describe the experimental data of the mono- and multielement systems (Table 2), and their parameters were obtained using nonlinear regression and the sum of squares of the errors (SSE). Table S1 (Supplementary Information section) shows that the experimental data were better applied to the Sips model, except for cadmium ions, which best fit the Langmuir model.

It can be seen in Table 7 that the CS 15% showed good adsorption capacity when compared to other adsorbents, which may be related to the experimental conditions and to the structure of the CS 15%, as well as to the affinity

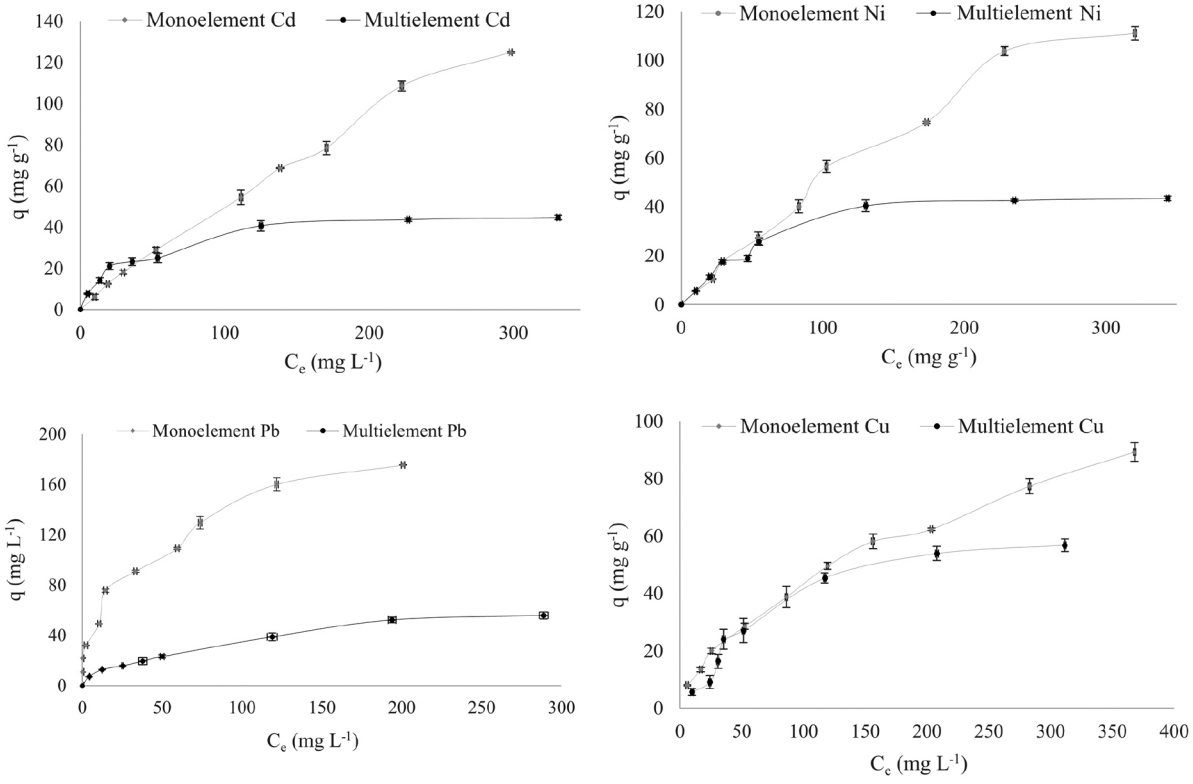

Figure 7. Comparison of experimental metal ions adsorption isotherms in mono- and multielement systems on CS 15%. W = 0.05 g; T = 28 ± 2 ºC; pH = 5.5.

Table 7. Comparison of different lignin-based adsorbent materials for metal ion removal

Adsorbent	Q_{max} / (mg g^{-1})				pH	Reference
	Ni^{II}	Cu^{II}	Cd^{II}	Pb^{II}		
CS 15%	179.9	307.6	480.0	493.0	5.5	this study
Polyethyleneimine-porous corn straw (PEI-PCS)	–	85.5	–	–	4.5	37
SiO_2-G1.0-Silica anchored	–	30.5	–	–	6.0	35
Cellulose acetate-polyethyleneimine-ethylenediamine (CAPE)	–	6.9		2.0	4.0	38
Carboxymethyl cellulose (CMC)	240.0	271.0		–	–	39
Pistachio shell	–	–	51.2	–	6.0	40
Peanut shells	–	–	62.1	–	6.0	40
Almond shells	–	–	78.7	–	6.0	40
Caryocar coriaceum Wittm bark	–	26.9	–	106.4	5.5	19,20
Mercerized delignified hemp stalks	–	–	–	283.3	5.0	41

CS: Castor (*Ricinus communis* L.) stalks. Q_{max}: maximum adsorption capacity.

of the metal ions by the functional groups present on the adsorbent surface.

FTIR spectra of CS, CS 15% before and after adsorption (saturated adsorbent) are shown in Figure 8.

In general, it can be observed a decrease and even exclusion of some bands after activation and saturation of the adsorbent. In CS 15%, there was a loss of the hemicellulose and lignin constituents, as demonstrated by the decrease in the intensity of bands 1511 cm^{-1} (aromatic ring) and 1251 cm^{-1} (CO stretching in acetyl groups of hemicelluloses) as well as the disappearance of the 1730 cm^{-1} band (stretching in CO). The saturation of the adsorbent also promoted a decrease in the bands due to binding with metallic ions. These alterations possibly indicate that ions were bound to the functional groups in the adsorbent (CS 15%), promoting the reduction of the initial signal as it probably makes the bond less susceptible to vibration.

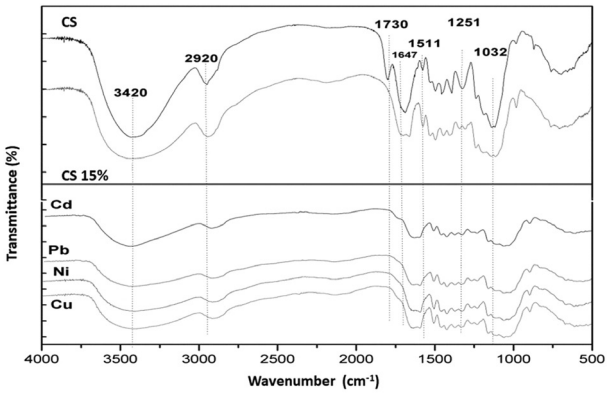

Figure 8. FTIR (ATR) spectra of CS before and after modification with 15% NaOH and before and after metal ion adsorption.

The results of the X-ray fluorescence analysis are presented in Table 8. The relative percentage of the elements remains similar in the CS and alkali CS adsorbents. However, the decrease in the elements present in the CS is noticeable when it is saturated, mainly Na and Ca. This exchange with the abovementioned ions is greater for Cu and Pb than for Ni and Cd. These results help explain the isotherms' results. In addition to the metal ions adsorption in the adsorbent organic sites, there are ionic exchanges in the pores of CS 15%.

The suggested adsorption mechanism is ion exchange and adsorption on organic sites in the adsorbent. The adsorption process involves the interaction between heavy metal species and functional groups of the adsorbent, such as hydroxyl and carboxyl. Additionally, the adsorption process is influenced by the presence of Na and Ca ions, which are

Table 8. Content of the elements based on X-ray fluorescence analysis

	CS	CS-15%	CS-15%-Ni	CS-15%-Cu	CS-15%-Cd	CS-15%-Pb
Na / %	30.21	29.32	1.90	0.68	10.07	0.61
Ca / %	62.10	62.65	19.75	3.43	19.62	5.55
Cl / %	1.09	1.09	–	–	–	–
Si / %	3.37	3.67	3.69	–	–	0.71
P / %	0.70	0.27	–	–	–	–
S / %	2.53	3.00	1.34	–	–	–
Ni / %	–	–	75.32	–	–	–
Cu / %	–	–	–	95.89	–	–
Cd / %	–	–	–	–	70.34	–
Pb / %	–	–	–	–	–	93.13

CS: Castor (*Ricinus communis* L.) stalks.

present in the adsorbent and can be exchanged for metal ions. The saturation of the adsorbent with heavy metals and the loss of some constituents, such as hemicellulose and lignin, suggest the formation of complexes between the metal ions and functional groups of the adsorbent.[42]

Based on that, chemisorption is the primary adsorption mechanism involved in the studied process, which was expected, since the CS materials are reported to have low BET (Brunauer, Emmett and Teller) specific area (16.53 $m^2 g^{-1}$).[43]

Desorption study

Using ultrapure water and buffer solution did not result in the desorption of evaluated metal ions (not shown). The adsorption capacities from the first to the fifth cycle for all metal ions were slightly altered, Ni (29.07-28.67 mg g^{-1}), Cu (33.87-33.02 mg g^{-1}), Cd (29.03-28.54 mg g^{-1}), and Pb (27.24-26.87 mg g^{-1}). Thus, within the studied regeneration and reuse cycles, CS 15% still has a slightly close initial adsorption capacity, indicating that the eluent and its concentration do not affect the adsorption sites. Therefore, it is effective in the desorption of the ions.

Hydrochloric acid showed maximum desorption efficiency in the first cycle, decreasing slightly over the cycles (Figure 9). The elution of metal ions occurs by replacing hydrogen ions from the acid. In the present study, nickel and copper ions had the lowest desorption percentages. According to He and Chen,[44] this may be due to their higher binding energies with adsorption sites containing oxygen atoms, making desorption difficult.

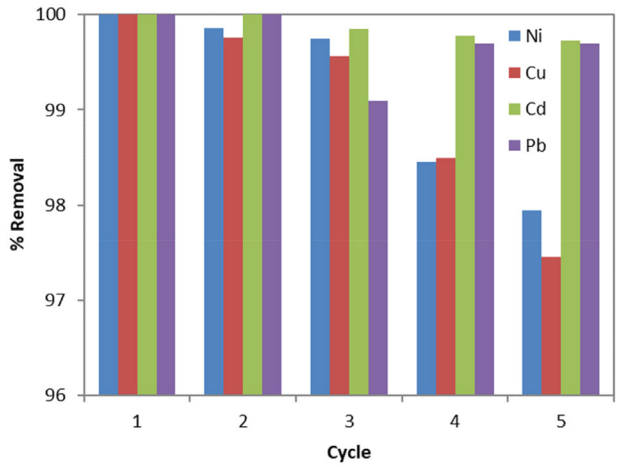

Figure 9. Percentage of desorbed metal ions from CS 15%.

Conclusions

The best activation occurred with 15% NaOH. The X-ray technique was used to observe the CS-presented type-II cellulose. The infrared spectra showed which surface groups (hydroxyl, carboxyl) are responsible for the ions' adsorption. X-ray fluorescence analysis confirmed the adsorption of metals and the ionic exchange mechanism. The experimental design demonstrated the correlation of the different variables and the influence of each factor on the adsorption of Ni, Cu, Cd, and Pb. In general, approximately 15 min are required for CS 15% saturation. X-ray fluorescence results indicated an ion exchange mechanism in the adsorption process.

The adsorption isotherm experimental data fit the Sips model better, confirming the heterogeneous surface, as shown in the infrared spectrum. Based on the data presented, the CS adsorbent is highly effective for treating water containing Ni, Cu, Cd, and Pb ions. After the saturation of CS 15%, the metal ions can be recovered, and the adsorbent can be regenerated through elution with an acidic solution (0.1 mol L^{-1} HCl). Five cycles of sorption/desorption were carried out, and a negligible loss in sorption capacity and physical degradation was observed. Among them, nickel and copper ions exhibited the lowest desorption percentages, likely due to their higher binding energies with adsorption sites containing oxygen atoms, making their desorption more challenging. These findings provide insights into the desorption behavior of metal ions and suggest that hydrochloric acid is effective in the desorption process.

Supplementary Information

Supplementary information is available free of charge at http://jbcs.sbq.org.br as PDF file.

Author Contributions

Diego Q. Melo was responsible for the conceptualization, data curation, formal analysis, funding acquisition, investigation, methodology, and writing original draft; Lucas F. Amorim for the data curation, formal analysis and writing review and editing; Juliene T. Oliveira for the conceptualization and data curation; André H. B. de Oliveira for the conceptualization and data curation; André G. de Oliveira for the data curation and writing original draft; João A. N. da Cunha Junior for the data curation; Carla B. Vidal for the writing review and editing; Ronaldo F. Nascimento for the conceptualization, project administration, resources, writing original draft, review and editing.

References

1. Vidal, C. B.; Melo, D. Q.; Raulino, G. S. C.; Luz, A. D.; Luz, C.; Nascimento, R. F.; *Desalin. Water Treat.* **2016**, *57*, 9001. [Crossref]

2. Zabihi, M.; Omidvar, M.; Motavalizadehkakhky, A.; Zhiani, R.; *Korean J. Chem. Eng.* **2022**, *39*, 367. [Crossref]
3. Raulino, G. S. C.; Silva, L. S.; Vidal, C. B.; Almeida, E. S.; Melo, D. Q.; Nascimento, R. F.; *J. Appl. Polym. Sci.* **2018**, *135*, 45879. [Crossref]
4. Herrera-Barros, A.; Bitar-Castro, N.; Villabona-Ortíz, A.; Tejada-Tovar, C.; González-Delgado, D. A.; *Sustainable Chem. Pharm.* **2020**, *17*, 100299. [Crossref]
5. Dinari, M.; Mokhtari, N.; Hatami, M.; *J. Polym. Res.* **2021**, *28*, 119. [Crossref]
6. Hamami, Z.; Javanbakht, V.; *Ceram. Int.* **2021**, *47*, 24170. [Crossref]
7. Al-Yousef, H. A.; Alotaibi, B. M.; Aouaini, F.; Sellaoui, L.; Bonilla-Petriciolet, A.; *J. Mol. Liq.* **2021**, *331*, 115697. [Crossref]
8. Saralegui, A. B.; Willson, V.; Caracciolo, N.; Piol, M. N.; Boeykens, S. P.; *J. Environ. Manage.* **2021**, *289*, 112398. [Crossref]
9. Neris, J. B.; Luzardo, F. H. M.; García, F.; da Silva, E. G. P.; Velasco, F. G.; *Chem. Eng. J.* **2019**, *357*, 404. [Crossref]
10. Santos, P. F.; Neris, J. B.; Luzardo, F. H. M.; Velasco, F. G.; Tokumoto, M. S.; da Cruz, R. S. J.; *Environ. Chem. Eng*. **2019**, *7*, 103363. [Crossref]
11. de Almeida, O. N.; Menezes, R. M.; Nunes, L. S.; Lemos, V. A.; Luzardo, F. H. M.; Velasco, F. G.; *Environ. Technol. Innovation* **2021**, *21*, 101336. [Crossref]
12. Neris, J. B.; Luzardo, F. H. M.; Santos, P. F.; de Almeida, O. N.; Velasco, F. G.; *J. Environ. Chem. Eng.* **2019**, *7*, 102885. [Crossref]
13. Wang, B.; Wu, K.; Liu, T.; Cheng, Z.; Liu, Y.; Liu, Y.; Niu, Y.; *J. Hazard. Mater.* **2023**, *442*, 130121. [Crossref]
14. Zambrano, G. B.; de Almeida, O. N.; Duarte, D. S.; Velasco, F. G.; Luzardo, F. H. M.; Nieto-González, L.; *Res. Eng.* **2022**, *13*, 100340. [Crossref]
15. Santana, C. S.; de Almeida, O. N.; Luzardo, F. H. M.; Tokumoto, M. S.; Velasco, F. G.; *Environ. Technol. Innovation* **2020**, *17*, 100534. [Crossref]
16. Correia, I. K. S.; Santos, P. F.; Santana, C. S.; Neris, J. B.; Luzardo, F. H. M.; Velasco, F. G.; *J. Environ. Chem. Eng.* **2018**, *6*, 2319. [Crossref]
17. Luzardo, F. H. M.; Velasco, F. G.; Alves, C. P.; Correia, I. K. S.; Cazorla, L. L.; *Rev. Bras. Eng. Agric. Ambient.* **2015**, *19*, 77. [Crossref]
18. Tran, H. V.; Nguyen, H. V.; Vu, D. V.; Le, T. D.; Nguyen, B. T.; Le, D. H.; *Korean J. Chem. Eng.* **2022**, *39*, 431. [Crossref]
19. Menezes, J. M. C.; Bento, A. M. S.; Filho, F. J. P.; Costa, J. G. M.; Coutinho, H. D. M.; Teixeira, R. N. P.; *Sustainable Chem. Pharm.* **2021**, *19*, 100364. [Crossref]
20. Menezes, J. M. C.; Bento, A. M. S.; Silva, J. H.; Filho, F. J. P.; Costa, J. G. M.; Coutinho, H. D. M.; Teixeira, R. N. P.; *Chemosphere* **2020**, *261*, 128144. [Crossref]
21. Wang, T.; Zheng, J.; Liu, H.; Peng, Q.; Zhou, H.; Zhang, X.; *Environ. Sci. Pollut. Res.* **2021**, *28*, 13800. [Crossref]
22. Melo, D. Q.; Vidal, C. B.; da Silva, A. L.; Teixeira, R. N. P.; Raulino, G. S. C.; Medeiros, T. C.; Fechine, P. B. A.; Mazzeto, S. E.; de Keukeleire, D.; Nascimento, R. F.; *J. Appl. Polym. Sci.* **2014**, *131*, 40883. [Crossref]
23. Box, G. E.; Hunter, W.G.; Hunter, J. S.; In *Statistics for Experimenters: An Introduction to Design, Data Analysis, and Model Building*, vol. 1; Wiley: New York, USA, 1972.
24. Melo, D. Q.; Sousa Neto, V. O.; Barros, F. C. F.; Raulino, G. S. C.; Vidal, C. B.; Nascimento, R. F.; *J. Appl. Polym. Sci.* **2016**, *133*, 43286. [Crossref]
25. Chen, S.; Zhong, M.; Wang, H.; Zhou, S.; Li, W.; Wang, T.; Li, J.; *Int. J. Environ. Sci. Technol.* **2023**, *20*, 1551. [Crossref]
26. *Minitab*, version 17; Minitab, Inc., Pennsylvania, United States, 2013.
27. Cooney, D. O.; *Adsorption Design for Wastewater Treatment*; Lewis Publishers: Boca Raton, US, 1999.
28. Crank, J.; *Mathematics of Diffusion*, 2nd ed.; Oxford University Press: Oxford, UK, 1975.
29. Langmuir, I.; *J. Am. Chem. Soc.* **1918**, *40*, 1361. [Crossref]
30. Freundlich, H. M. F.; *J. Phys. Chem.* **1906**, *57*, 385.
31. Sips, R.; *J. Chem. Phys.* **1948**, *16*, 490. [Crossref]
32. Gong, J.; Li, J.; Xu, J.; Xiang, Z.; Moa, L.; *RSC Adv.* **2017**, *7*, 33486. [Crossref]
33. Gheibi, M.; Eftekhari, M.; Tabrizi, M. G.; Fathollahi-Fard, A. M.; Tian, G.; *Int. J. Environ. Sci. Technol*. **2022**, *19*, 6429. [Crossref]
34. Nouacer, I.; Hammadi, S.; Benalia, M.; Djedid, M.; Bencheikh, S. E.; *S. Afr. J. Bot.* **2023**, *157*, 297. [Crossref]
35. Wu, K.; Wang, B.; Tang, B.; Luan, L.; Xu, W.; Zhang, B.; Niu, Y.; *Chinese Chem. Lett.* **2022**, *33*, 2721. [Crossref]
36. Bayuo, J.; Rwiza, M.; Mtei K.; *RSC Adv.* **2022**, *12*, 11233. [Crossref]
37. Zhu, C.; Wang, W.; Wu, Z.; Zhang, X.; Chu, Z.; Yang, Z.; *Int. J. Biol. Macromol.* **2023**, *233*, 123595. [Crossref]
38. Huang, Z.; Huang, Z.; Feng, L.; Luo, X.; Wu, P.; Cui, L.; Mao, X.; *Carbohydr. Polym.* **2018**, *202*, 470. [Crossref]
39. Zhang, R.; Liu, B.; Ma, J.; Zhu, R.; *Eur. Polym. J.* **2022**, *179*, 111577. [Crossref]
40. Kayranli, B.; *Alexandria Eng. J.* **2022**, *61*, 443. [Crossref]
41. Liu, J.; Zhang, C.; Tao, B.; Beckerman, J.; *J. Taiwan Inst. Chem. Eng.* **2023**, *143*, 104701. [Crossref]
42. Bayuo, J.; Rwiza, M. J.; Sillanpää, M.; Mtei, K. M.; *RSC Adv.* **2023**, *19*, 12634. [Crossref]
43. Ferreira, L. M.; de Melo, R. R.; Pimenta, A. S.; Azevedo, T. K. B.; de Souza, K. P.; *Biomass Convers. Biorefin.* **2022**, *12*, 1181. [Crossref]
44. He, J.; Chen, J. P.; *Bioresour. Technol.* **2014**, *160*, 67. [Crossref]

Submitted: March 23, 2023
Published online: July 6, 2023